

A neo-sex chromosome in the Monarch butterfly, *Danaus plexippus*

James R. Walters* and Andrew J. Mongue

Department of Ecology and Evolutionary Biology, University of Kansas, Lawrence, KS, USA

*Author for correspondence: James R Walters, Department of Ecology and Evolutionary Biology, University of Kansas, Lawrence, KS, USA
phone: 785-864-6341
email: jrwalters@ku.edu

Abstract

We report the discovery of a neo-sex chromosome in Monarch butterfly, *Danaus plexippus*, and several of its close relatives. Z-linked scaffolds in the *D. plexippus* genome assembly were identified via sex-specific differences in Illumina sequencing coverage. Additionally, a majority of the *D. plexippus* genome assembly was assigned to chromosomes based on counts of 1-to-1 orthologs relative to the butterfly *Melitaea cinxia* (with replication using two other Lepidopteran species), where genome scaffolds have been robustly mapped to linkage groups. Combining sequencing-coverage based Z-linkage with homology based chromosomal assignments provided strong evidence for a Z-autosome fusion in the *Danaus* lineage, involving the autosome homologous to chromosome 21 in *M. cinxia*. Coverage analysis also identified three notable assembly errors resulting in chimeric Z-autosome scaffolds. The timing of this Z-autosome fusion event currently remains ambiguous due to incomplete sampling of karyotypes in the Danaini tribe of butterflies. The discovery of a neo-Z and the provisional assignment of chromosome linkage for >90% of *D. plexippus* genes lays the foundation for novel insights concerning sex chromosome evolution in this increasingly prominent female-heterogametic model species for functional and evolutionary genomics.

Background

Major rearrangements of karyotype and chromosome structure often have substantial evolutionary impacts on both the organisms carrying such mutations and the genes linked to such genomic reorganization [1, 2]. Additionally, such large-scale chromosomal mutations often present novel opportunities to investigate molecular evolutionary and functional genetic processes. One prominent example of this is the evolution of neo-sex chromosomes, which can arise from the fusion of an autosome with an existing and well-differentiated allosome. This effectively instantaneous transformation of a formerly autosomal set of genes into sex-linked loci is fertile ground for comparative analyses aimed at understanding the distinct set of evolutionary forces acting on sex chromosomes relative to autosomes [3-6]. Furthermore, when the relevant taxa also happen to be tractable genetic model systems, there is opportunity to explore the functional and mechanistic changes associated with sex chromosome evolution. The congruence of neo-sex chromosomes existing in a model system is relatively rare, although there are some notable examples.

Numerous independent origins of neo-sex chromosomes are known in *Drosophila* fruit flies, where recent work has revealed much about the evolutionary and functional dynamics of these unusual sequences [3, 7-11]. Substantial insights have also come from stickleback fish, where neo-sex chromosomes appear to play an important role in reproductive isolation between incipient species [12-14]. Looking beyond these established model systems, the rapid expansion of genomic technologies has allowed extensive analyses of gene content, sex-biased gene expression, dosage compensation, and sequence divergence for recently evolved sex chromosomes among a very diverse set of organisms. This includes, for example, several insect lineages [Teleostid flies, a grasshopper, and Strepsiptera [15-17]], vertebrates [mammals and

birds [4, 18, 19], and plants [*Silene* and *Rumex* genera [20-22]]. A clear consensus emerges from this research that the lack of recombination associated with sex chromosomes catalyzes a cascade of evolutionary changes involving the degeneration of one allosome, the accumulation of genes with sex-biased expression, increased evolutionary rates, and (often, but not always) the acquisition of dosage compensation. Yet many of the details in this process remain elusive and unresolved, including the rate of allosome divergence, the role of positive selection versus drift, the importance sex-specific selection, and the mechanisms underlying dosage compensation (or the reasons for its absence). It is therefore important to continually identify new opportunities for novel insight into the evolution of sex chromosomes.

Overwhelmingly, research on sex chromosomes occurs in male-heterogametic (XY) species [5, 23-25]. This appears to be particularly true for neo-sex chromosomes, where contemporary genomic analyses of neo-Z or neo-W chromosomes are currently lacking [with one notable exception for birds [4]]. This imbalance is unfortunate, as ZW sex determination replaces male-specific selection with female-specific selection during the evolution of heterogamety, offering a novel framework for elucidating sex chromosome evolution. What prospects are there for improving this situation? Birds are the most prominent vertebrate taxon that is female-heterogametic, but it appears that avian neo-sex chromosomes are quite rare, and absent from prominent model species (*e.g.*, chicken, zebra finch) [26, 27]. Fishes and squamates seem to be far more labile in sex-chromosome constitution, with numerous independent transitions between male and female-heterogamety and relatively frequent sex-autosome fusions [28], thus there are potentially great opportunities in these taxa. However, no obviously tractable ZW model system with neo-sex chromosomes is yet apparent for these lineages.

For many reasons, Lepidoptera (moths and butterflies) may be the most promising female-heterogametic taxon for studying neo-sex chromosomes. Synteny is unusually well-conserved in Lepidoptera [29-31], yet there are also numerous known examples of independently evolved neo-Z and neo-W chromosomes, several of which have been well-characterized cytogenetically [6, 32-34]. Furthermore, comparative genomic resources in this insect order are substantial and growing quickly (www.lepbase.org).

In this context, we report the fortuitous discovery of a neo-Z chromosome in the monarch butterfly, *Danaus plexippus*, and closely related species. Monarch butterflies, renowned for their annual migration across North America, already have a strong precedent as a model system in ecology [35]. Recently monarchs have emerged as a model system for genome biology, with a well-assembled reference genome, extensive population resequencing data, and a precedent for genome engineering [36-38]. The discovery of a neo-Z chromosome substantially enriches the value of this species as a research model in genome biology and lays the foundation for extensive future insights into the evolution and functional diversity of sex chromosomes.

Results

Identifying Z-linked scaffolds in *D. plexippus*

We identified Z-linked scaffolds in the *D. plexippus* genome assembly [36, 39] by comparing sequencing coverage from male and female samples. Z chromosome DNA content in males should be twice that in females, while autosomes should have equal DNA content between sexes. Thus a corresponding two-fold difference in sequencing coverage is expected between sexes for the Z chromosome, but not autosomes, and can be used to identify Z-linked scaffolds [16, 40, 41]. A histogram of male:female ratios of median coverage clearly identifies two clusters of scaffolds (Fig. 1). One large cluster is centered around equal coverage between sexes ($\text{Log}_2 \text{ M:F} = 0$) and a second, smaller cluster is centered around two-fold greater coverage in males ($\text{Log}_2 \text{ M:F} = 1$). We can thus clearly distinguish the Z-linked scaffolds as those with $\text{Log}_2(\text{M:F}) > 0.5$, with the remainder of the scaffolds presumed to be autosomal.

One scaffold, DPSCF300028, appeared to have an intermediate coverage ratio, falling at $\text{Log}_2 \text{ M:F} \approx 0.7$. One likely explanation for such intermediate values is that the scaffold is a chimera of Z-linked and autosomal sequence arising from an error in genome assembly [41]. In this scenario, only a portion of the scaffold is Z-linked and gives a two-fold difference in coverage between sexes; the remaining autosomal fraction of the scaffold yields equal coverages. The resulting estimate of average coverage for the entire scaffold then falls at an intermediate value between expectations for Z or autosomal scaffolds. This is clearly true for DPSCF300028, as revealed by examining basepair-level sequencing coverage across the scaffold (Fig. 2A). While average male coverage is consistent across the entire length of the scaffold, female coverage exhibits a clear transition between coverage equal to males (the autosomal portion) and coverage one half that of males (the Z-linked portion). Indeed, there are two such transitions in scaffold DPSCF300028, which we estimate to occur at 0.76 Mbp and 1.805 Mbp, creating a “sandwich” of one Z segment flanked by autosomal segments.

Ortholog counts link scaffolds to chromosomes.

Lepidoptera show a very high level of conserved synteny across substantial evolutionary divergences [29-31]. Thus it is possible to use counts of orthologous genes to assign *D. plexippus* scaffolds to linkage groups (i.e. chromosomes) delineated in other moth or butterfly species. We generated predicted orthologs between *D. plexippus* and three other reference species where genetic linkage mapping has been used to assign genomic scaffolds to chromosomes: *Melitaea cinxia* (N=31), *Heliconius melpomene* (N=21), and *Bombyx mori* (N=28) [29, 30, 42]. *M. cinxia* and *H. melpomene* are both nymphalid butterflies equally diverged from *D. plexippus*, while the silkworm, *B. mori*, is distinctly more divergent [43, 44].

To assign *D. plexippus* scaffolds to chromosome, we tabulated per scaffold the counts of one-to-one reference species orthologs per reference species chromosome. *D. plexippus* scaffolds were then assigned to the reference chromosome with the maximum count of orthologs. For a few scaffolds, a tie occurred in maximum ortholog count per reference chromosome, in which case the scaffold was removed from further analysis; at most this occurred for only 14 scaffolds per reference species and usually involved small scaffolds

harboring fewer than 5 orthologs. Typically this method yielded a clear “best” reference chromosomal assignment for each *D. plexippus* scaffold.

This method of ortholog-count chromosomal “lift-over” resulted in putative chromosomal assignments for >90% of *D. plexippus* genes relative to each reference species (Table 1, Supplementary Table S1). Also, at least 4500 orthologous genes were co-localized to chromosome between *D. plexippus* and each reference species. Having several thousand orthologs mapped to chromosome in *D. plexippus* and a reference species presents the opportunity to examine the extent of chromosomal rearrangements and gene movement between the two species. Here we primarily report the comparison with *M. cinxia* because this species is believed to retain the ancestral lepidopteran karyotype of 31 chromosomes [29]. Furthermore, this count of chromosomes is closest to that reported for *Danaus* butterflies (N=30), indicating it is likely the most similar karyotype to *D. plexippus* [45]. *H. melpomene* and *B. mori* are known to have more derived karyotypes involving several chromosomal fusions relative to *M. cinxia*; details of comparisons to these two species are reported in the supplementary content and provide comparable support for the primary findings reported here.

Figure 3 summarizes the cross-tabulation of chromosomal linkage for >4500 orthologs between *M. cinxia* and *D. plexippus*. The overwhelming majority of orthologs fall on the diagonal, indicating substantial conservation of chromosomal linkage and relatively little gene shuffling, as has been reported elsewhere for Lepidoptera [29-31]. The two most notable exceptions to this pattern both involve the Z chromosome (Chr1). In one case [McChr9, DpChr1] we could anticipate this because of the previously identified chimeric scaffold, DPSCF300028. This scaffold harbors 34 orthologs assigned to McChr1 and 23 orthologs assigned to McChr9, consistent with the chimeric nature of the scaffold revealed from male:female coverage ratios (Fig 2A).

The second case [McChr1, DpChr21] appeared to arise entirely from a single scaffold, DPSCF300001, the largest scaffold in the *D. plexippus* v3 assembly. This scaffold carried 107 orthologs assigned to McChr21, 28 orthologs assigned to McChr1, 13 orthologs assigned to McChr23, and a few other orthologs assigned to other autosomes. Notably, despite the large number of apparently autosomal orthologs, the average male:female coverage ratio for DPSCF300001 was consistent with it being Z-linked [$\text{Log}_2(\text{M:F coverage}) = 0.92$]. Nonetheless, we plotted coverage across the chromosome and detected a ~1 Mbp portion at the 3’ end of the scaffold with coverage patterns consistent with being an autosome (Fig 2C). The *M. cinxia* orthologs in this autosomal portion were linked exclusively to McChr23. There was not an obvious shift in sequencing coverage between sexes to indicate a misassembled Z-autosome chimera involving McChr21. Rather, it appeared that nearly the entirety of scaffold DPSCF300001 had twice the coverage in males than in females, consistent with the entire scaffold being Z-linked, both for regions apparently homologous to Mc1(Z) and McChr21.

A neo-Z chromosome in *D. plexippus*

The observation that a substantial portion of scaffold DPSCF300001 was Z-linked and homologous to McChr21, while another large section of the same scaffold was homologous to McChr1 (i.e., McChrZ), led us to hypothesize that a single Z-autosome fusion could explain the

karyotypic differences between *D. plexippus* (N=30) and *M. cinxia* (N=31). To further investigate this hypothesis of a major evolutionary transition in sex chromosome composition in the *Danaus* lineage, we examined the chromosomal assignments for all Monarch scaffolds identified as Z-linked via sequencing coverage ratios (Z-cov scaffolds). Specifically, we identified the unique set of reference chromosomes to which Z-cov scaffolds were assigned, and then examined the male:female coverage ratio for all scaffolds assigned to those reference chromosomes. In the case of *M. cinxia* as the reference, all Z-cov scaffolds were assigned either to McChr1 or McChr21 (Fig. 4; comparable results were obtained for *H. melpomene* and *B. mori*, Supplementary Fig. S2). This result provides further evidence that the Z in *D. plexippus* is a neo-sex chromosome reflecting the fusion of the ancestral Z chromosome with an autosome homologous to McChr21.

This analysis intersecting Z-cov scaffolds with homology to *M. cinxia* revealed two scaffolds that did not fit with the expected pattern of sequencing coverage (Fig. 4). First, scaffold DPSCAF300044 was assigned to McChr1(Z) but had $\text{Log}_2 \text{ M:F} \approx 0.25$, much more like other autosomes than other Z-linked chromosomes. This scaffold had seven Z-linked orthologs and 4 autosomal, suggesting another chimeric scaffold. Indeed, examining coverage across the scaffold revealed a clear transition in coverage as previously observed for DPSCF300001 and DPSCF300028 (Fig 2B). Thus the low male:female coverage ratio for this scaffold is the artifact of an assembly error. Again we were able to partition the scaffold into two sections, one autosomal and one Z-linked, with a breakpoint estimated at 0.29 Mbp.

DPSCF300403 was the other scaffold where the M:F ratio of median coverage was inconsistent with the hypothesis of a neo-Z chromosome. This scaffold was assigned to McChr21 but had an autosomal coverage ratio. Coverage along the chromosome was consistent with it being entirely autosomal (Supplementary Figure S3). In this case the scaffold carried only a single one-to-one orthologous gene (and only 5 protein-coding genes total), so the assignment to McChr21 is tenuous and likely inaccurate. This scaffold also had a single one-to-one ortholog found in *B. mori*, and none identified in *H. melpomene*. We therefore consider this scaffold largely uninformative concerning the presence of a neo-Z in *D. plexippus*.

The neo-Z chromosome exists in the Monarch's close relatives

The Monarch population genomic data set of Zha *et al.* (2014) also contained male and female resequencing samples for four closely related congeners: *D. gilippus*, *D. chrysippus*, *D. erippus*, and *D. eresimus*. This presented the opportunity to assess whether this neo-Z exists in these species in addition to Monarch. Published reports of an N=30 karyotype in some of these species leads to the strong prediction that they all also carry the same neo-Z chromosomal arrangement [45]. As expected, male versus female sequence coverage analysis does clearly show the same scaffolds homologous to both McChr1 and McChr21 as having sequencing coverage consistent with a neo-Z (Fig. 5). Thus it appears that the origin of this neo-Z predates the diversification of the genus *Danaus*.

Annotating chromosomal linkage

The combination of sequencing coverage analysis and comparative “liftover” allowed us to provisionally assign most genes to chromosomes in *D. plexippus*. Genes falling on Z-cov scaffolds, or within the portion assessed as Z-linked for noted chimeric scaffolds, have been assigned to the Z chromosome. We further partitioned these Z-linked genes into being on the ancestral (anc-Z) or neo (neo-Z) portion of the Z, based on scaffold homology to reference chromosomes. In the case of DPSCF300001, we localized the fusion point between anc-Z and neo-Z by aligning *M. cinxia* and *H. melpomene* scaffolds from the Z (HmChr21, McChr1) or relevant autosome (HmChr2, McChr21). Alignments with both species were consistent in placing the fusion point at approximately 3.88 Mbp (Supplementary Fig. S4). Otherwise, genes and scaffolds were assigned to chromosomes based directly on the results of the “lift-over” relative to *M. cinxia*. Table 2 gives a tabulated summary of results, while results for every protein coding gene are provided in Supplementary Table S3.

Discussion

This discovery of a neo-Z chromosome in *Danaus* butterflies and our discrimination of genes falling on the ancestral versus recently autosomal portions are fundamental observations that provide the foundation for a host of future inferences. These results create novel opportunities to address rates of molecular evolution, the evolution of dosage compensation, the pattern of allosome divergence, and many other important questions in sex chromosome biology, all in an emerging genetic and genomic female-heterogametic model system.

It seems evident from the results presented here that if there remains a neo-W chromosome (*i.e.*, a degraded homolog of the neo-Z segment), it must be substantially diverged from the neo-Z. We infer this from the very consistent 2:1 coverage ratio observed on scaffold regions corresponding to McChr21. If the neo-W retained substantial homology to the neo-Z, we would expect many sequencing reads emanating from the neo-W to align to the neo-Z, and shift this ratio towards equality. This evidently does not occur, strongly indicating substantial divergence between the neo-Z and any neo-W sequence that is retained. Indeed, it is not even clear at this point whether there is any neo-W chromosome at all. This is an obvious point for immediate investigation, perhaps best approached using cytogenetic techniques [6, 32].

Brown *et al.* (2004) report chromosome counts from male butterflies of several species from three genera in the Danaini butterfly tribe: *Danaus* (N=30), *Anetia* (N=31), and *Lycorea* (N=30). The most recent phylogenetic study of these species reports *Anetia* within the most basally diversifying lineage in this group [46]. So it is tempting to speculate that the Z-autosome fusion reported here for *Danaus* occurred within the Danaini, after the divergence from *Anetia*, which has 31 chromosomes, presumably reflecting a shared ancestral karyotype with *Melitaea*. However, the same phylogenetic study reports *Anetia* as sister to *Lycorea* (N = 30), within the same basally splitting lineage. Because no other chromosome counts are known for the numerous species at intermediate divergences between *Danaus* and the (*Anetia*,*Lycorea*) lineage, we are left with two plausible scenarios, assuming the reported phylogenetic relationships are accurate. In one case, *Anetia* indeed retains the ancestral karyotype while fusions independently occurred in *Lycorea* and also in the lineage leading to *Danaus*. The alternative case is that a Z-autosome fusion predates the origins of all Danaini, with a

subsequent chromosomal fission in *Anetia*, producing one extra chromosome for $N=31$, a chromosome count that is convergent but not homologous to *Melitaea*. Resolving these two possibilities will likely require a comparative analysis of Z-chromosome homology within the *Danaini*.

In analyzing patterns of chromosomal fusion in *H. melpomene* and *B. mori* relative to *M. cinxia*, Ahola *et al.* (2014) report a significant tendency for a limited set of ancestral chromosomes – particularly the smallest ones – to be involved in chromosomal fusion events. Neither the ancestral Z nor McChr21 are among these small, repeatedly fused chromosomes. Thus the chromosomal fusion reported here does not fit neatly with the pattern described by Ahola *et al.* Nonetheless, HmChr2 (homologous to McChr21) is the second smallest chromosome that remains unfused between these lineages [47]. So it is also difficult to argue strongly that this Z-autosome fusion in *Danaus* is a striking contrast to the trend of chromosomal fusions involving small chromosomes.

Conclusion

We have used a combination of genome sequencing coverage and comparative genomic analysis to demonstrate that *Danaus* butterflies harbor a neo-Z chromosome resulting from the fusion of the ancestral Z chromosome and an autosome homologous to Chr21 in *M. cinxia*. Our analysis also identified and resolved several Z-autosome chimeric scaffolds in the most recent assembly of the *D. plexippus* genome. This discovery and provisional assignment of chromosome linkage for >90% of *D. plexippus* genes paves the way for myriad and diverse investigations into sex chromosome evolution, which are likely to be of distinct importance given the increasing prominence of monarch butterfly as a female-heterogametic model species for functional and evolutionary genomics.

Methods

Sequencing coverage analysis

Illumina shotgun genomic DNA sequencing data for three male and three female *D. plexippus* individuals were selected for analysis from samples sequenced by Zhan *et al.* (2014) [38]. Male-female pairs were selected on the basis of approximately equal sequencing coverage. Samples were aligned to the *D. plexippus* version 3 genome assembly with bowtie2 (v2.1.0), using the “very sensitive local” alignment option [39, 48]. The resulting alignments were parsed with the *genomecov* and *groupby* utilities in the BedTools software suite (v2.17.0) to obtain a per-base median coverage depth statistic for each scaffold [49]. Genomic sequencing data from other *Danaus* species, also generated by Zhan *et al.* 2014, were aligned to the same assembly using Stampy (v1.0.22) (default parameters, except for *substitutionrate=0.1*) [50]. Details of all sample identity, including GenBank SRA accessions, are given in Supplementary Table S2.

Coverage analyses comparing males and females were limited to scaffolds of lengths equal to or greater than the N90 scaffold (160,499 bp) [39]. Also, incomplete cases were

excluded (i.e., scaffolds with no reads from one or more samples). In total, 140 scaffolds were excluded, leaving 5,257 scaffolds analyzed. For each sample, each scaffold's median coverage was divided by the mean across all scaffold median coverages, thereby normalizing for differences in overall sequencing depth between samples. Samples were grouped by sex and the per-scaffold mean of normalized coverage depth was compared between sexes, formulated as the log2 of the male:female coverage ratio. Autosomal scaffolds are expected to exhibit equal coverage between sexes, yielding a log2 ratio of zero. Z linked scaffolds should have a ratio of one, due to the two-fold greater representation in males. Manipulation, analysis, and visualization of coverage data was performed using custom R scripts [51].

For select scaffolds with intermediate median coverage ratios, we used Bedtools *genomecov* to calculate per-base coverage, in order to identify potential assembly errors producing Z-Autosomal chimeric scaffolds. For each sample, coverage per base was divided by the mean of all scaffold median coverages, thus normalizing for overall sequencing depth. The normalized coverage per base was averaged (mean) within sex and visualized along the length of the scaffold by using the median of a 5kbp sliding window, shifted by 1kbp steps.

Point estimates for Z-autosomal break points in chimeric scaffolds were generated using a sliding window analysis of male:female coverage ratios. Putative break points were obtained as the maximum of the absolute difference between adjacent non-overlapping windows. A window of 150 Kbp with 10 kbp steps was used for DPSCF300001 and the 5' break point of DPSCF30028. A window of 10 kbp with 1 kbp steps was used for DPSCF30044 and in a second, localized analysis between 1.5 Mb and the 3' terminus of DPSCF30028 to localize the second, 3' break point.

Orthology-based chromosomal assignments for *D. plexippus* scaffolds.

Putative chromosomal linkage was predicted for *D. plexippus* scaffolds relative to the genome assemblies of three reference species, *M. cinxia*, *B. mori*, and *H. melpomene*, based on counts of orthologous genes [29, 30, 42]. Orthologous proteins were predicted between *D. plexippus* and each reference species using the *Proteinortho* pipeline [52]. Using only 1-to-1 orthologs, we tabulated per *D. plexippus* scaffold the number of genes mapped to each chromosome in the reference species. Each *D. plexippus* scaffold was tentatively assigned to the chromosome with the highest count of orthologs in the reference species. Scaffolds were excluded from analysis when maximum ortholog count was tied between two or more scaffolds, though this situation was rare and always involved scaffolds with low counts of (orthologous) genes.

Point estimate of the Z-autosome fusion

The fusion point in Monarch between ancestrally Z and autosomal segments was localized by aligning the homologous *H. melpomene* or *M. cinxia* chromosomes against Monarch scaffold DPSCF300001 [29, 47]. Alignments were based on six-frame amino acid translations using the PROmer algorithm and visualized with mummerplot, both from the MUMmer software package (v3.1) [53]. We initially aligned the complete set of scaffolds from the Z (HmChr21, McChr1) or relevant autosome (HmChr2, McChr21), yielding a preliminary indication that the Z-A fusion point occurred at ~4 Mbp on DPSCF300001. To refine and better visualize this phenomenon, "pseudo-assemblies" were created for each chromosome using query scaffolds producing >500

bp of total aligned coverage on DPSCF300001. Selected query scaffolds were concatenated into a single fasta entry, with ordering based on target alignment positions. For each species, the Z and autosomal pseudo-assemblies were co-aligned to DPSCF300001. The transition point between contiguous alignments of the two pseudo-assemblies was interpreted as the approximate location of the Z-A in Monarch.

Acknowledgements

This manuscript is dedicated to Chip Taylor, Ann Ryan, and the many hard-working members of MonarchWatch.org. Jim Mallet and John Davey provided helpful comments on this work. This research was supported by NSF-DEB 1457758 (to J.R.W.). The computing for this project was performed on the Community Cluster at the Center for Research Computing at the University of Kansas.

Author contributions: JRW conceived and designed research, performed analyses, and drafted the manuscript. AJM performed analyses and helped draft the manuscript. Both authors read and approved the final manuscript.

Competing Interests: The authors (JRW & AJM) declare no competing interests.

Additional data files:

Monarch_neoZ_Gene-Scaff.xlsx contains predicted chromosomal linkage, where determined, for all *D. plexippus* protein coding genes.

Works Cited

1. Lynch M: *The Origins of Genome Architecture*. Sunderland, MA: Sinauer Associates Incorporated; 2007.
2. Soltis P, Soltis DE: *Polyploidy and Genome Evolution*. New York, NY: Springer Science & Business Media; 2012.
3. Bachtrog D, Jensen JD, Zhang Z: **Accelerated adaptive evolution on a newly formed X chromosome**. *PLoS Biol* 2009, **7**:e82.
4. Pala I, Hasselquist D, Bensch S, Hansson B: **Patterns of molecular evolution of an avian neo-sex chromosome**. *Molecular Biology and Evolution* 2012, **29**:3741–3754.
5. Bachtrog D: **Y-chromosome evolution: emerging insights into processes of Y-chromosome degeneration**. *Nat Rev Genet* 2013, **14**:113–124.
6. Šíchová J, Nguyen P, Dalíková M, Marec F: **Chromosomal Evolution in Tortricid Moths: Conserved Karyotypes with Diverged Features**. *PLoS ONE* 2013, **8**:e64520.
7. Counterman BA, Ortíz-Barrientos D, Noor MAF: **Using comparative genomic data to test for fast-X evolution**. *Evolution* 2004, **58**:656–660.
8. Flores SV, Evans AL, McAllister BF: **Independent origins of new sex-linked chromosomes in the melanica and robusta species groups of Drosophila**. *BMC Evol Biol* 2008, **8**:33.
9. Zhou Q, Ellison CE, Kaiser VB, Alekseyenko AA, Gorchakov AA, Bachtrog D: **The Epigenome of Evolving Drosophila Neo-Sex Chromosomes: Dosage Compensation and Heterochromatin Formation**. *PLoS Biol* 2013, **11**:e1001711.
10. Brown EJ, Bachtrog D: **The chromatin landscape of Drosophila: comparisons between species, sexes, and chromosomes**. *Genome Res* 2014, **24**:1125–1137.
11. Nozawa M, Fukuda N, Ikeo K, Gojobori T: **Tissue- and Stage-Dependent Dosage Compensation on the Neo-X Chromosome in Drosophila pseudoobscura**. *Molecular Biology and Evolution* 2014, **31**:614–624.
12. Kitano J, Ross JA, Mori S, Kume M, Jones FC, Chan YF, Absher DM, Grimwood J, Schmutz J, Myers RM, Kingsley DM, Peichel CL: **A role for a neo-sex chromosome in stickleback speciation**. *Nature* 2009, **461**:1079–1083.
13. White MA, Kitano J, Peichel CL: **Purifying Selection Maintains Dosage-Sensitive Genes during Degeneration of the Threespine Stickleback Y Chromosome**. *Molecular Biology and Evolution* 2015, **32**:1981–1995.
14. Yoshida K, Makino T, Yamaguchi K, Shigenobu S, Hasebe M, Kawata M, Kume M, Mori S, Peichel CL, Toyoda A, Fujiyama A, Kitano J: **Sex Chromosome Turnover Contributes to Genomic Divergence between Incipient Stickleback Species**. *PLoS Genet* 2014, **10**:e1004223.
15. Baker RH, Wilkinson GS: **Comparative Genomic Hybridization (CGH) Reveals a Neo-X Chromosome and Biased Gene Movement in Stalk-Eyed Flies (Genus Teleopsis)**. 2010:1–14.
16. Mahajan S, Bachtrog D: **Partial Dosage Compensation in Strepsiptera, a Sister Group of Beetles**. *Genome Biology and Evolution* 2015, **7**:591–600.

17. Palacios-Gimenez OM, Marti DA, Cabral-de-Mello DC: **Neo-sex chromosomes of *Ronderosia bergi*: insight into the evolution of sex chromosomes in grasshoppers.** *Chromosoma* 2015, **124**:353–365.
18. Zhou Q, Wang J, Huang L, Nie W-H, Wang J-H, Liu Y, Zhao X-Y, Yang F-T, Wang W: **Neo-sex chromosomes in the black muntjac recapitulate incipient evolution of mammalian sex chromosomes.** *Genome Biol* 2008, **9**:R98.
19. Murata C, Kuroki Y, Imoto I, Tsukahara M, Ikejiri N, Kuroiwa A: **Initiation of recombination suppression and PAR formation during the early stages of neo-sex chromosome differentiation in the Okinawa spiny rat, *Tokudaia muenninki*.** *BMC Evol Biol* 2015, **15**:234.
20. Papadopoulos AST, Chester M, Ridout K, Filatov DA: **Rapid Y degeneration and dosage compensation in plant sex chromosomes.** *Proceedings of the National Academy of Sciences* 2015, **112**:13021–13026.
21. Charlesworth D: **Plant contributions to our understanding of sex chromosome evolution.** *New Phytol* 2015, **208**:52–65.
22. Hough J, Hollister JD, Wang W, Barrett SCH, Wright SI: **Genetic degeneration of old and young Y chromosomes in the flowering plant *Rumex hastatulus*.** *Proceedings of the National Academy of Sciences* 2014, **111**:7713–7718.
23. Ellegren H: **Sex-chromosome evolution: recent progress and the influence of male and female heterogamety.** *Nat Rev Genet* 2011, **12**:157–166.
24. Parsch J, Ellegren H: **The evolutionary causes and consequences of sex-biased gene expression.** *Nat Rev Genet* 2013, **14**:83–87.
25. Vicoso B, Charlesworth B: **Evolution on the X chromosome: unusual patterns and processes.** *Nat Rev Genet* 2006, **7**:645–653.
26. Pala I, Naurin S, Stervander M, Hasselquist D, Bensch S, Hansson B: **Evidence of a neo-sex chromosome in birds.** *Heredity* 2012, **108**:264–272.
27. Nanda I, Schlegelmilch K, Haaf T, Scharf M, Schmid M: **Synteny conservation of the Z chromosome in 14 avian species (11 families) supports a role for Z dosage in avian sex determination.** *Cytogenet Genome Res* 2008, **122**:150–156.
28. Pennell MW, Kirkpatrick M, Otto SP, Vamori JC, Peichel CL, Valenzuela N, Kitano J: **Y fuse? Sex chromosome fusions in fishes and reptiles.** *PLoS Genet* 2015, **11**:e1005237.
29. Ahola V, Lehtonen R, Somervuo P, Salmela L, Koskinen P, Rastas P, Välimäki N, Paulin L, Kvist J, Wahlberg N, Tanskanen J, Hornett EA, Ferguson LC, Luo S, Cao Z, de Jong MA, Duplouy A, Smolander O-P, Vogel H, McCoy RC, Qian K, Chong WS, Zhang Q, Ahmad F, Haukka JK, Joshi A, Salojärvi J, Wheat CW, Grosse-Wilde E, Hughes D, et al.: **The *Glanville fritillaria* genome retains an ancient karyotype and reveals selective chromosomal fusions in *Lepidoptera*.** *Nature Communications* 2014, **5**:4737.
30. Heliconius Genome Consortium: **Butterfly genome reveals promiscuous exchange of mimicry adaptations among species.** *Nature* 2012, **487**:94–98.
31. Pringle EG, Baxter SW, Webster CL, Papanicolaou A, Lee SF, Jiggins CD: **Synteny and chromosome evolution in the lepidoptera: evidence from mapping in *Heliconius melpomene*.** *Genetics* 2007, **177**:417–426.
32. Nguyen P, Sýkorová M, Šíchová J, Kůta V, Dalíková M, Čapková Frydrychová R, Neven LG, Sahara K, Marec F: **Neo-sex chromosomes and adaptive potential in tortricid pests.** *Proceedings of the National Academy of Sciences* 2013, **110**:6931–6936.

33. Yoshido A, Sahara K, Marec F, Matsuda Y: **Step-by-step evolution of neo-sex chromosomes in geographical populations of wild silkmoths, *Samia cynthia* ssp.** *Heredity* 2010, **106**:614–624.
34. Traut W, Sahara K, Marec F: **Sex chromosomes and sex determination in Lepidoptera.** *Sex Dev* 2007, **1**:332–346.
35. Oberhauser KS, Solensky MJ: *Monarch Butterfly Biology & Conservation*. Ithaca, NY: Cornell University Press; 2004.
36. Zhan S, Merlin C, Boore JL, Reppert SM: **The Monarch Butterfly Genome Yields Insights into Long-Distance Migration.** *Cell* 2011, **147**:1171–1185.
37. Merlin C, Beaver LE, Taylor OR, Wolfe SA, Reppert SM: **Efficient targeted mutagenesis in the monarch butterfly using zinc-finger nucleases.** *Genome Res* 2013, **23**:159–168.
38. Zhan S, Zhang W, Niitepöld K, Hsu J, Haeger JF, Zalucki MP, Altizer S, de Roode JC, Reppert SM, Kronforst MR: **The genetics of monarch butterfly migration and warning colouration.** *Nature* 2014, **514**:317–321.
39. Zhan S, Reppert SM: **MonarchBase: the monarch butterfly genome database.** *Nucleic Acids Research* 2012, **41**:D758–D763.
40. Vicoso B, Emerson JJ, Zektser Y, Mahajan S, Bachtrog D: **Comparative Sex Chromosome Genomics in Snakes: Differentiation, Evolutionary Strata, and Lack of Global Dosage Compensation.** *PLoS Biol* 2013, **11**:e1001643.
41. Martin SH, Dasmahapatra KK, Nadeau NJ, Salazar C, Walters JR, Simpson F, Blaxter M, Manica A, Mallet J, Jiggins CD: **Genome-wide evidence for speciation with gene flow in *Heliconius* butterflies.** *Genome Res* 2013, **23**:1817–1828.
42. International Silkworm Genome Consortium: **The genome of a lepidopteran model insect, the silkworm *Bombyx mori*.** *Insect Biochem Mol Biol* 2008, **38**:1036–1045.
43. Wahlberg N, Leneveu J, Kodandaramaiah U, Peña C, Nylin S, Freitas AVL, Brower AVZ: **Nymphalid butterflies diversify following near demise at the Cretaceous/Tertiary boundary.** *Proceedings of the Royal Society B: Biological Sciences* 2009, **276**:4295–4302.
44. Kawahara AY, Breinholt JW: **Phylogenomics provides strong evidence for relationships of butterflies and moths.** *Proceedings of the Royal Society B: Biological Sciences* 2014, **281**:20140970–20140970.
45. Brown KS, Schoultz Von B, Suomalainen E: **Chromosome evolution in Neotropical Danainae and Ithomiinae (Lepidoptera).** *Heredity* 2004, **141**:216–236.
46. Brower AVZ, Wahlberg N, Ogawa JR, Boppré M, Vane-Wright RI: **Phylogenetic relationships among genera of danaine butterflies (Lepidoptera: Nymphalidae) as implied by morphology and DNA sequences.** *Systematics and Biodiversity* 2010, **8**:75–89.
47. Davey JW, Chouteau M, Barker SL, Maroja L, Baxter SW, Simpson F, Joron M, Mallet J, Dasmahapatra KK, Jiggins CD: **Major Improvements to the *Heliconius melpomene* Genome Assembly Used to Confirm 10 Chromosome Fusion Events in 6 Million Years of Butterfly Evolution.** *G3 (Bethesda)* 2016.
48. Langmead B, Salzberg SL: **Fast gapped-read alignment with Bowtie 2.** *Nat Methods* 2012, **9**:357–359.
49. Quinlan AR, Hall IM: **BEDTools: a flexible suite of utilities for comparing genomic features.** *Bioinformatics* 2010, **26**:841–842.

50. Lunter G, Goodson M: **Stampy: a statistical algorithm for sensitive and fast mapping of Illumina sequence reads.** *Genome Res* 2011, **21**:936–939.
51. R Development Core Team: **R: A Language and Environment for Statistical Computing.** 2014.
52. Lechner M, Findeiss S, Steiner L, Marz M, Stadler PF, Prohaska SJ: **Proteinortho: Detection of (Co-)orthologs in large-scale analysis.** *BMC Bioinformatics* 2011, **12**:124.
53. Kurtz S, Phillippy A, Delcher AL, Smoot M, Shumway M, Antonescu C, Salzberg SL: **Versatile and open software for comparing large genomes.** *Genome Biol* 2004, **5**:R12.

Table 1. Summary of assigning *D. plexippus* genes and scaffolds to chromosomes via orthology “liftover” relative to *M. cinxia*.

1:1 orthologs identified	6,740
1:1 orthologs assigned to <i>M. cinxia</i> chromosome	4,607 (68.4%)
Protein coding genes in <i>D. plexippus</i>	15,130
<i>D. plexippus</i> protein coding genes assigned to chromosome	14,129 (93.4%)
<i>D. plexippus</i> scaffolds putatively assigned to chromosomes	454

Table 2. Summary of provisional chromosomal linkage for *D. plexippus* protein coding genes, with chromosomal identity reflecting homology to *M. cinxia*

Chromosome	Number of Genes
1	1101
Anc-Z	624
Neo-Z	477
2	704
3	758
4	582
5	494
6	689
7	483
8	535
9	647
10	452
11	574
12	576
13	501
14	429
15	493
16	524
17	604
18	561
19	414
20	399
22	302
23	318
24	185
25	329
26	274
27	250
28	284
29	294
30	151
31	168
Not Assigned	1055

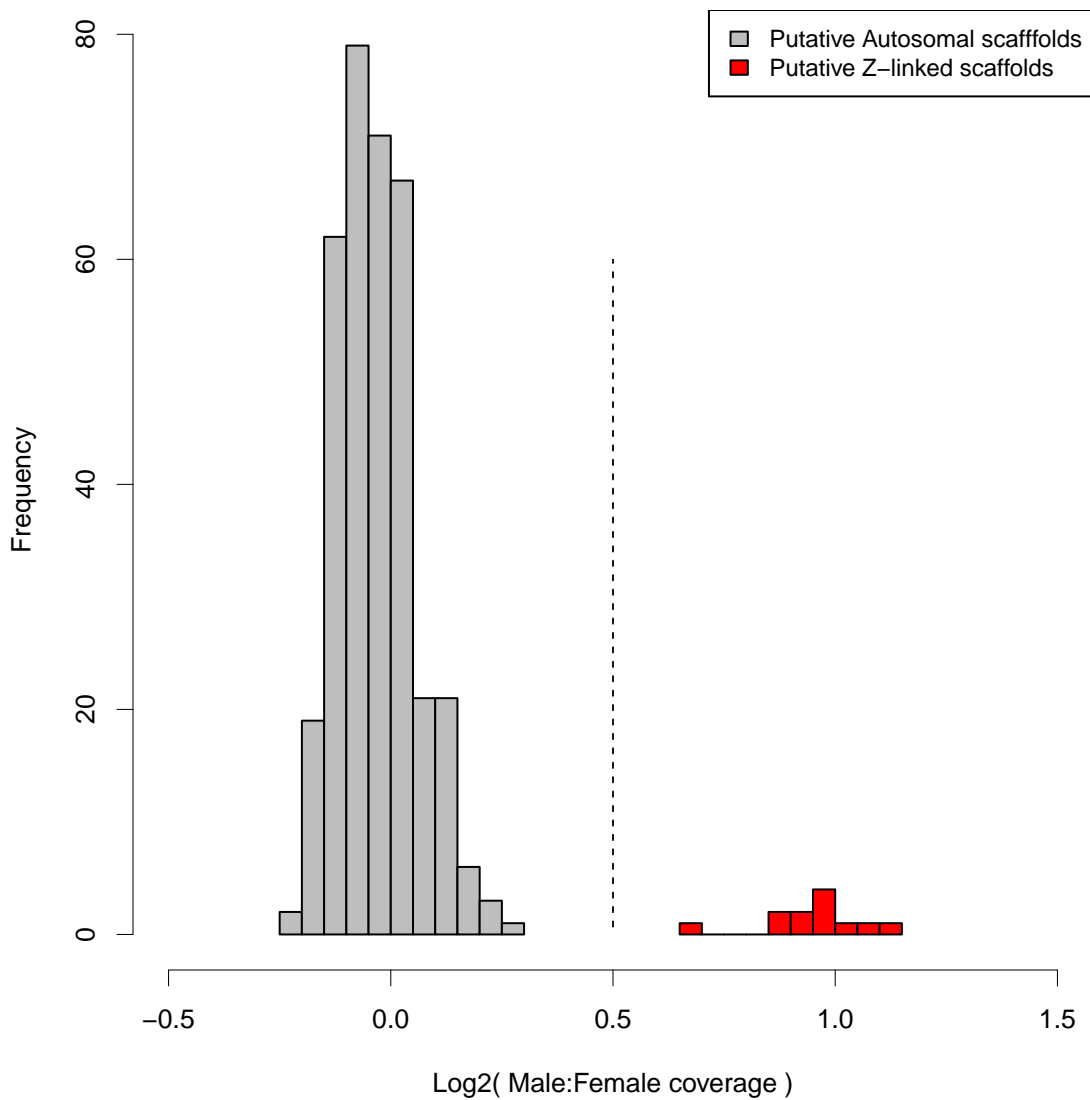
Figure 1. Distribution of median normalized male:female genomic sequencing coverage ratios for *D. plexippus* version 3 assembly scaffolds. Only scaffolds of length equal to or greater than the N90 scaffold are shown. The dotted line at 0.5 represents the value used to partition scaffolds as autosomal (grey) or Z-linked (red).

Figure 2. Normalized male and female coverage along the length of chimeric scaffolds, for (A) DPSCF300028, (B) DPSCF300044, and (C) DPSCF300001. Coverages are plotted as sliding windows (width = 5Kbp, step = 1 Kbp) of median basepair values. The associated male:female ratio of coverage for each window is plotted as a red line below the pair of sex-specific plots. Asterisks indicate the estimated break point between Z linked and autosomal segments of each scaffold, as determined by the maximum difference in adjacent, non-overlapping windows of male:female ratio (see methods for details).

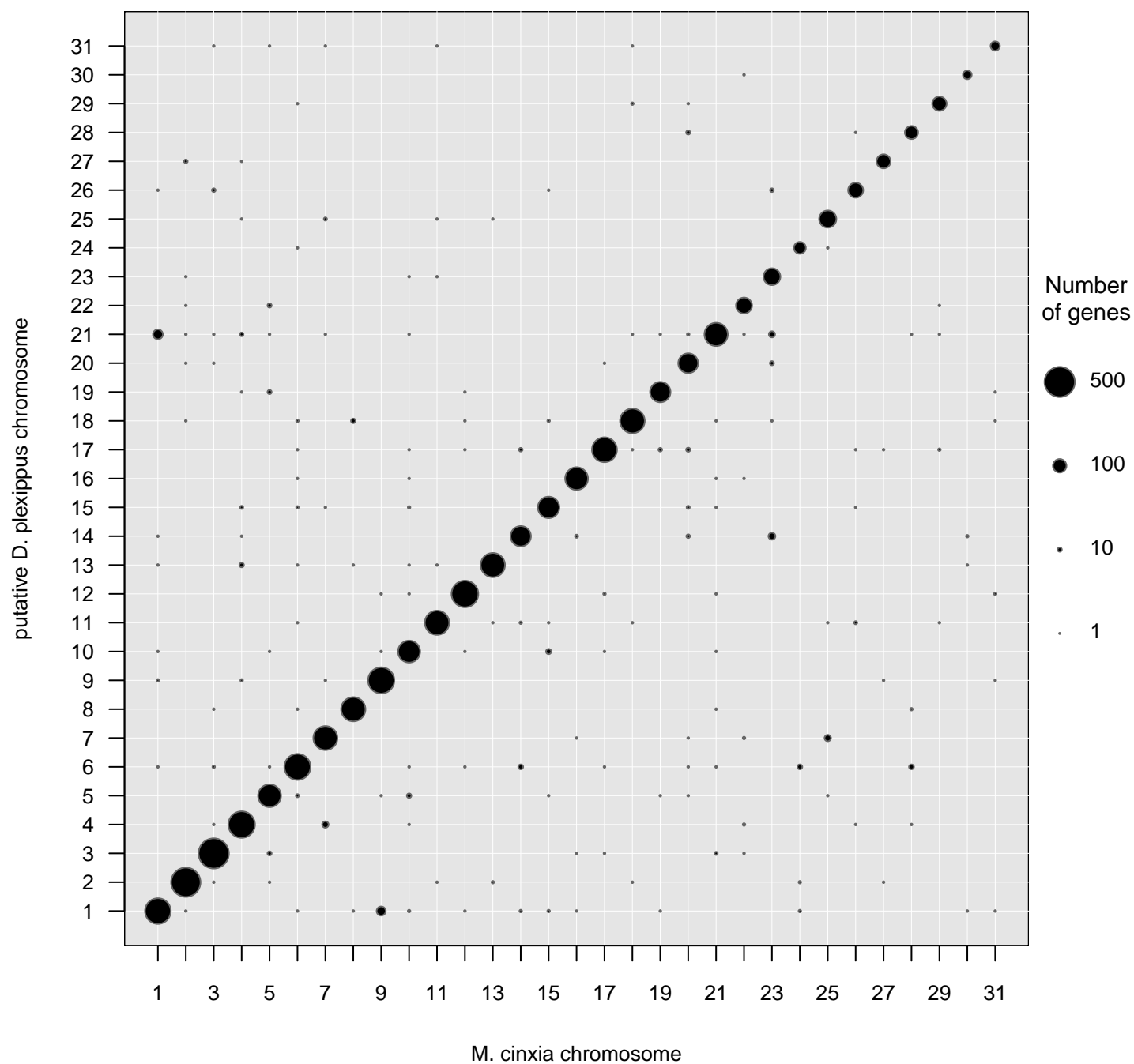
Figure 3. Chromosomal co-linkage between *D. plexippus* and *M. cinxia* for predicted orthologous proteins.

Figure 4. Ratios of male:female median normalized genomic sequencing coverage plotted by scaffold length. Scaffolds homologous via “liftover” procedure to *M. cinxia* chromosomes 1/Z (blue) and 21 (green) are plotted in distinct colors. Dotted lines indicate expected values for Z-linked (red) and autosomal (black) scaffolds.

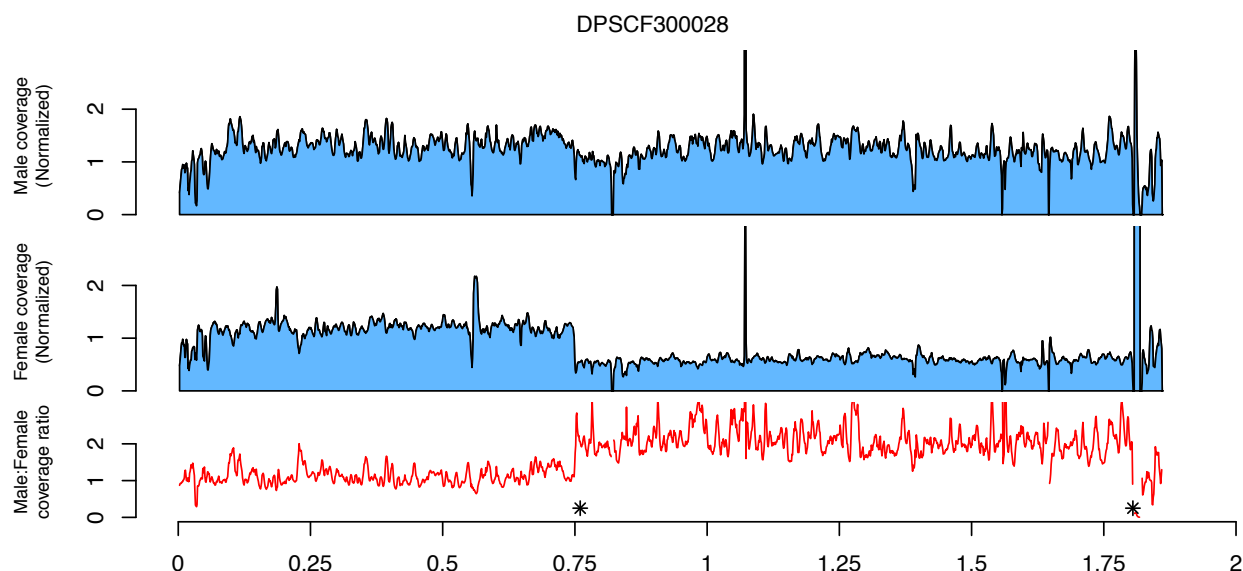
Figure 5. Ratios of male:female median normalized genomic sequencing coverage plotted by scaffold length for four species of *Danaus* butterflies.



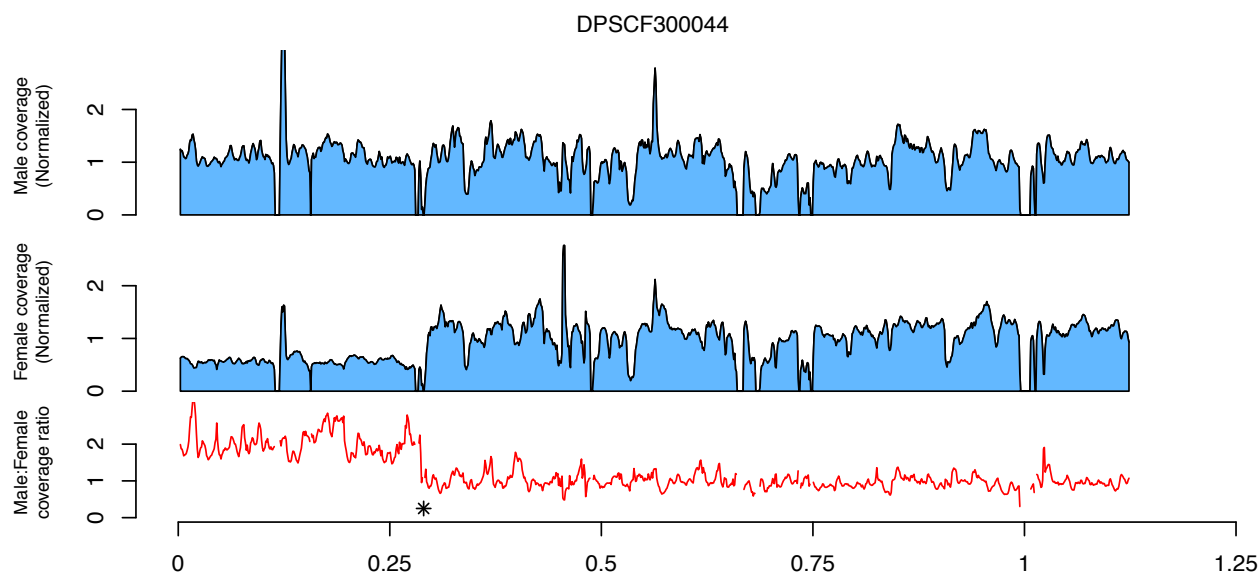
Ortholog Chromosomal Co-localization: *M. cinxia* vs. *D. plexippus*



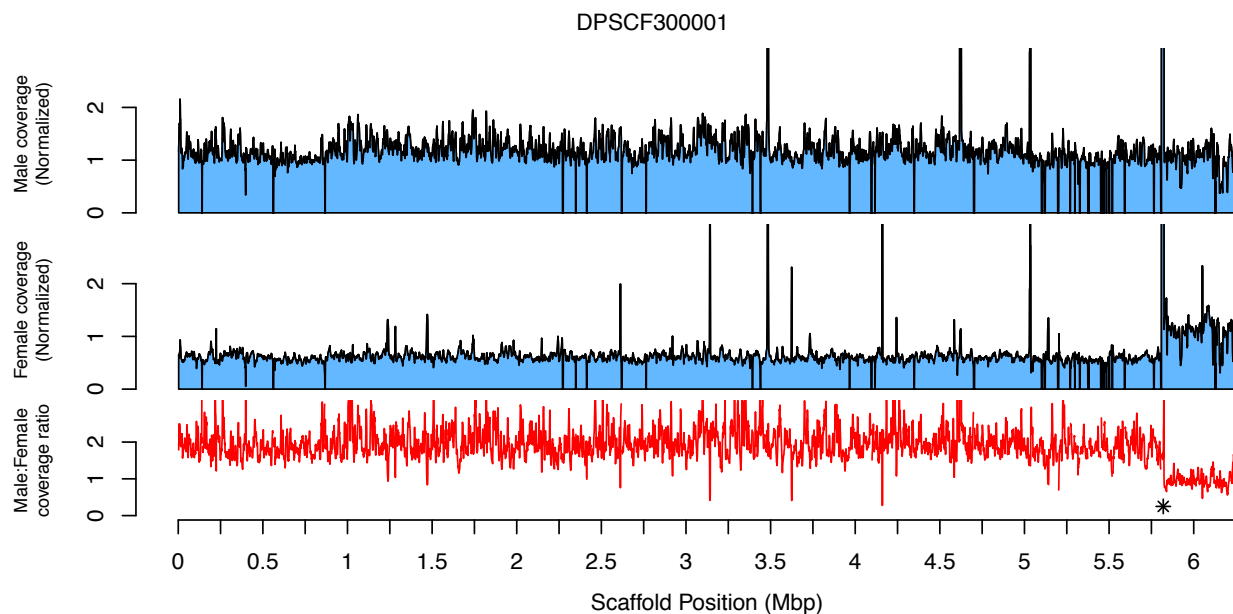
A

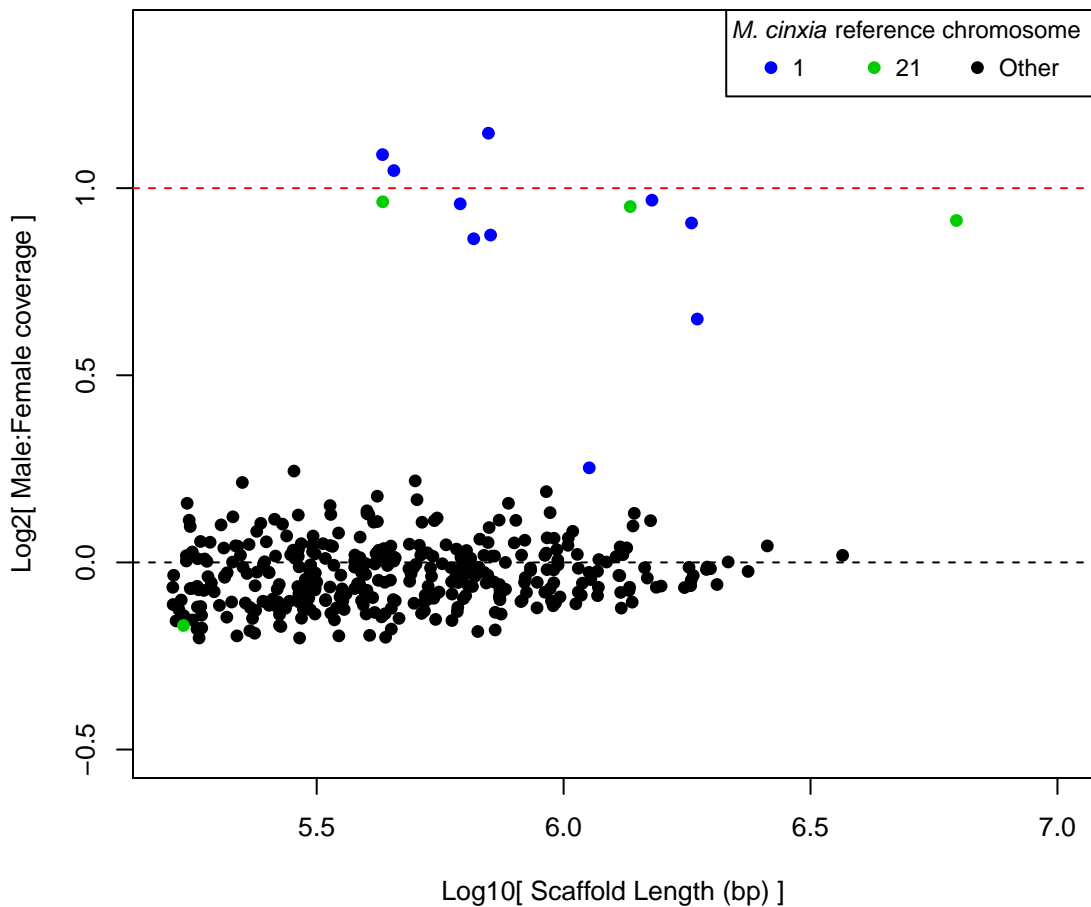


B

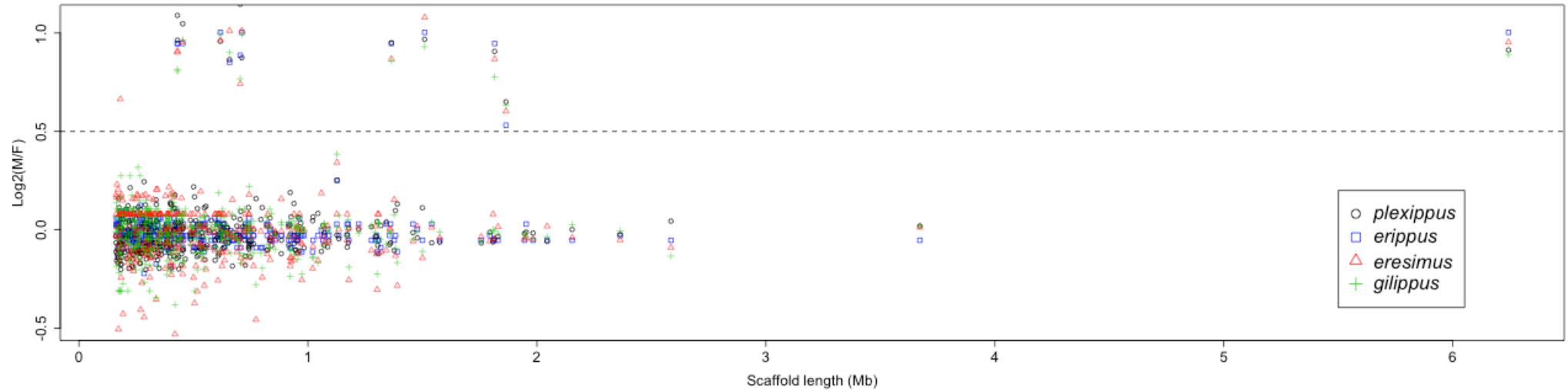


C

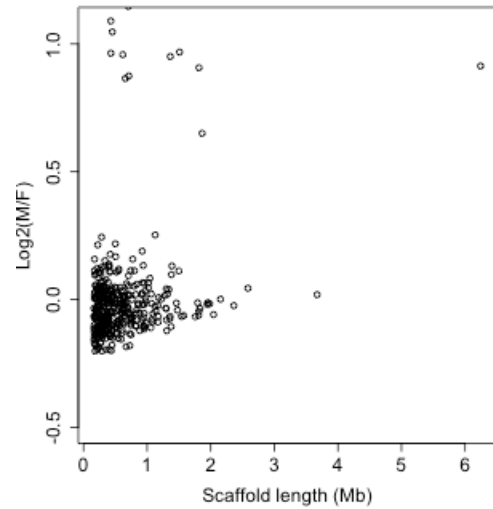




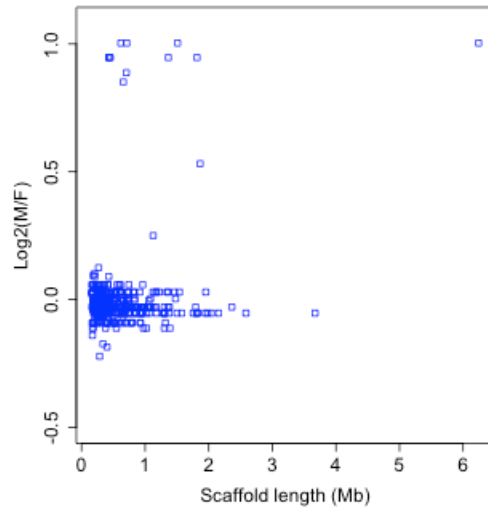
Danaus spp. median depth of coverage by scaffold



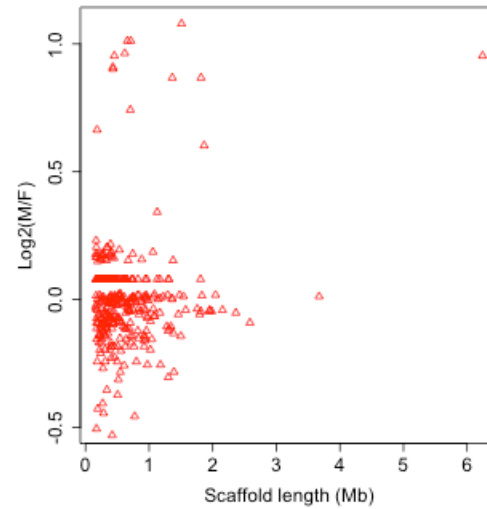
D. plexippus



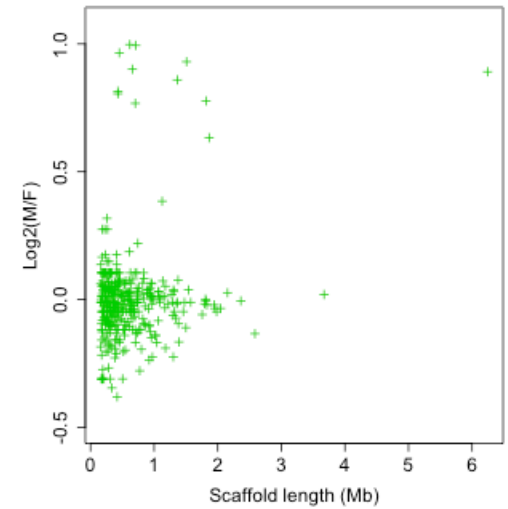
D. erippus



D. eresimus



D. gilippus



Macrosyteny: *B. mori* vs *D. plexippus*

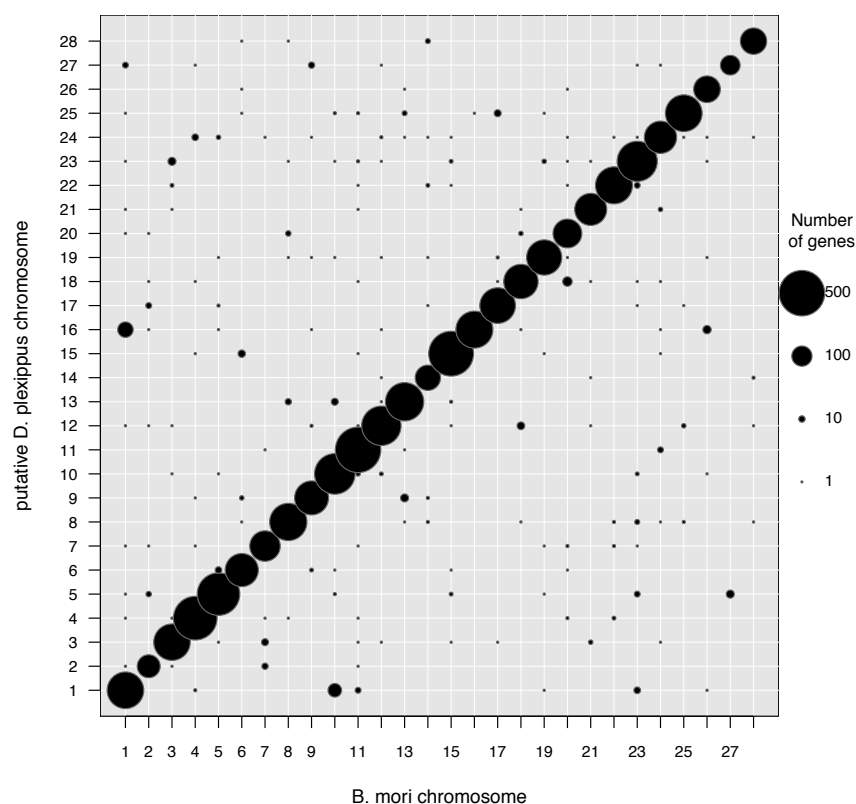
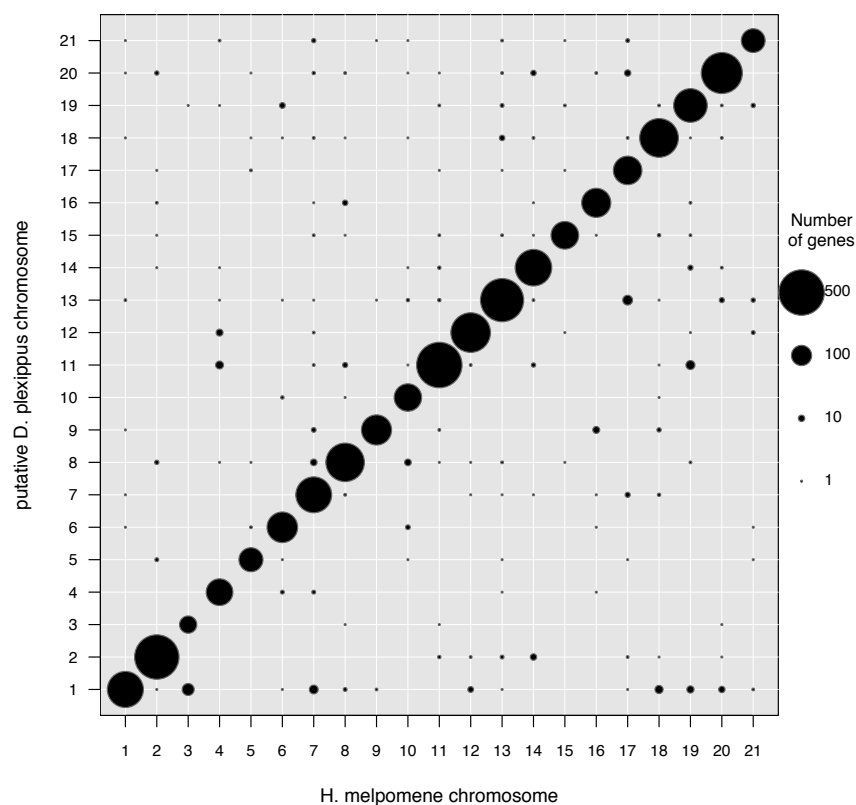


Figure S1. Chromosomal co-linkage between *D. plexippus* and *B. mori* (top) or *H. melpomene* (bottom) for predicted orthologous proteins.

Macrosyteny: *H. melpomene* vs *D. plexippus*



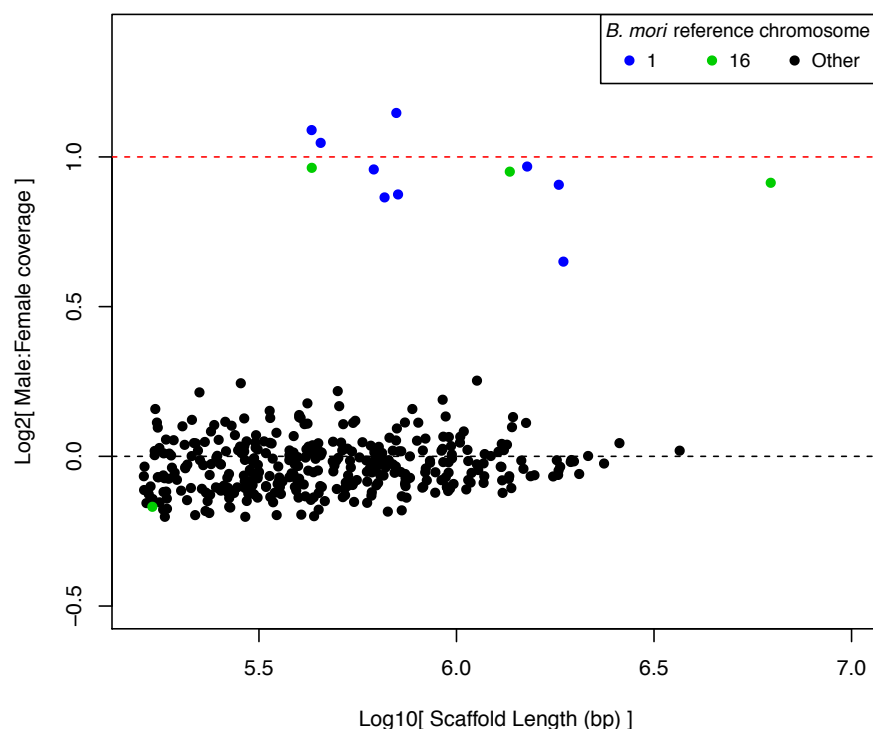
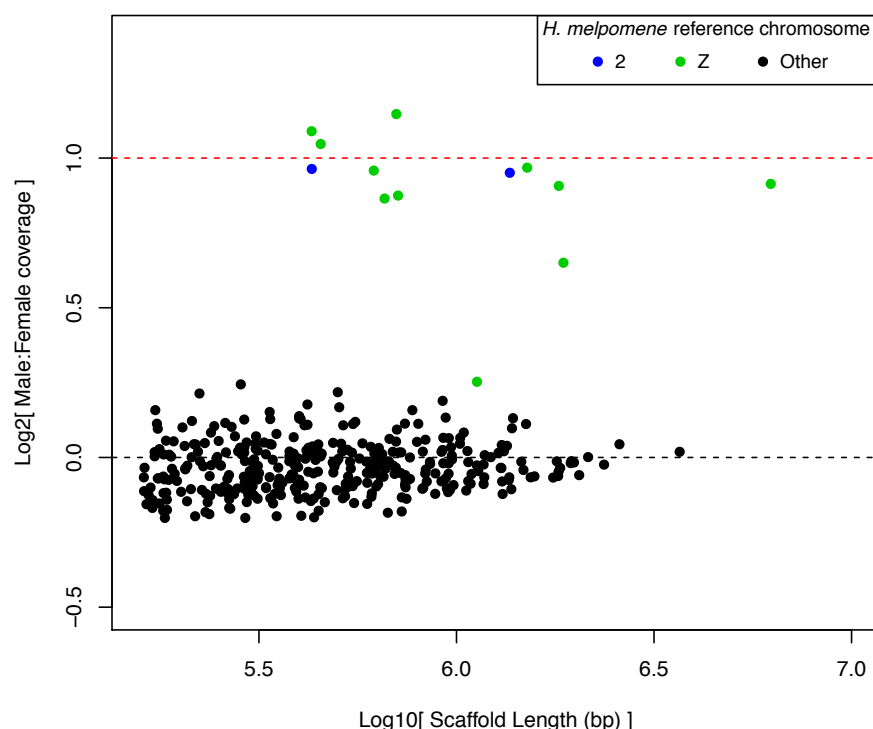


Figure S2. Ratios of male:female median normalized genomic sequencing coverage plotted by scaffold length. Scaffolds assigned to chromosomes putative homologous to the neo-Z chromosome in *D. plexippus* are plotted in distinct colors. Top, relative to *B. mori*, to chromosomes 1 (*i.e.*, Z ; blue) and 16 (green). Bottom, relative to *H. melpomene*, chromosomes 1 (*i.e.*, Z ; green) and 2 (blue).



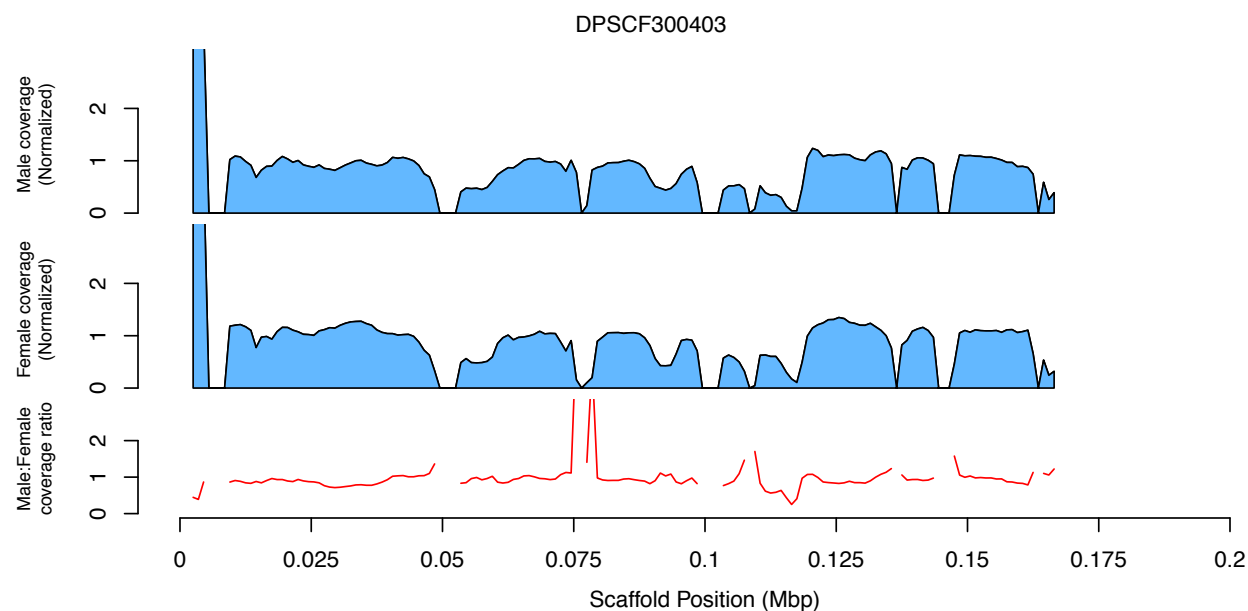


Figure S3. Normalized male and female coverage along the length DPSCF300403. Coverages are plotted as sliding windows (width = 5Kbp, step = 1 Kbp) of median basepair values. The associated male:female ratio of coverage for each window is plotted as a red line below the pair of sex-specific plots.

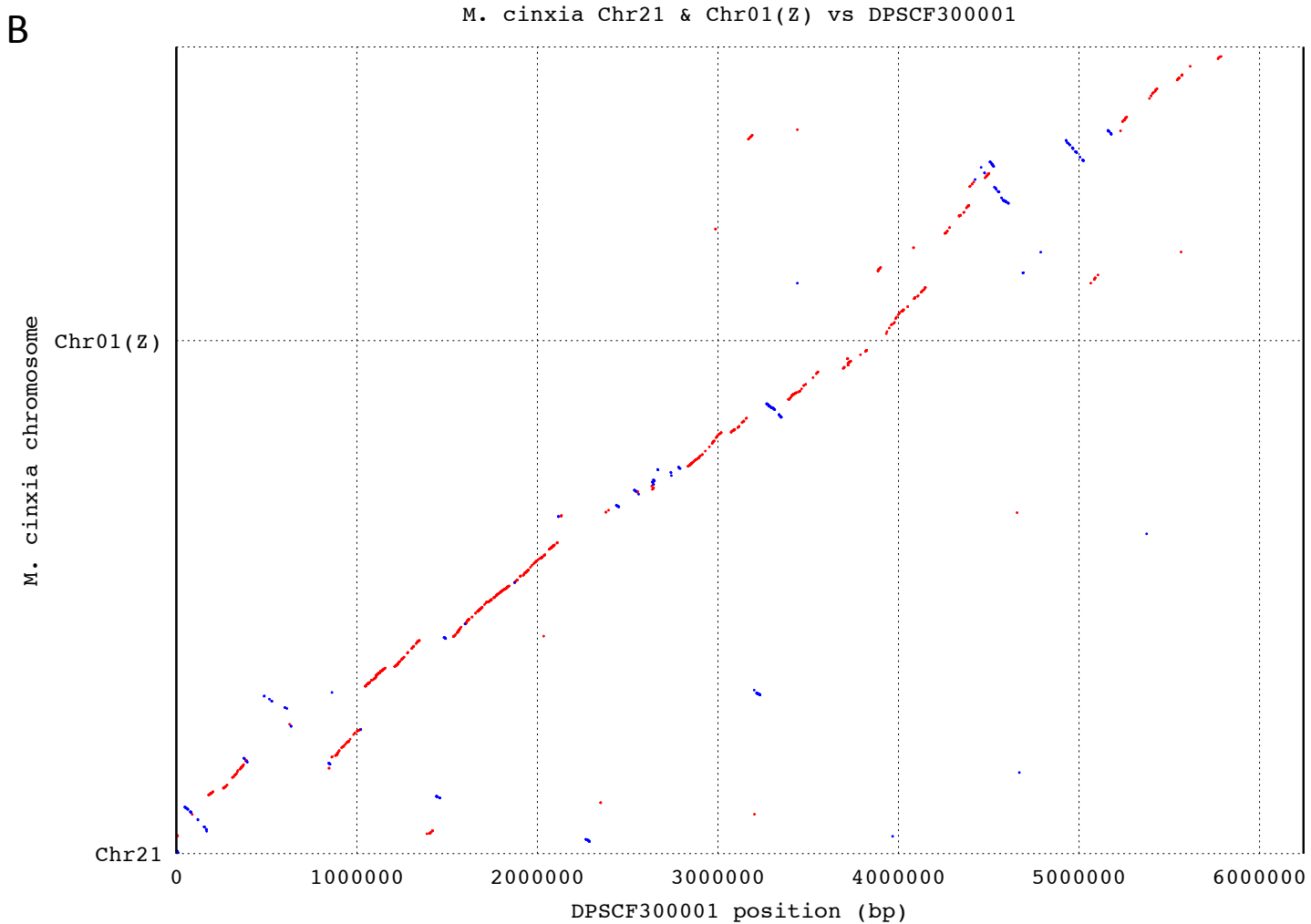
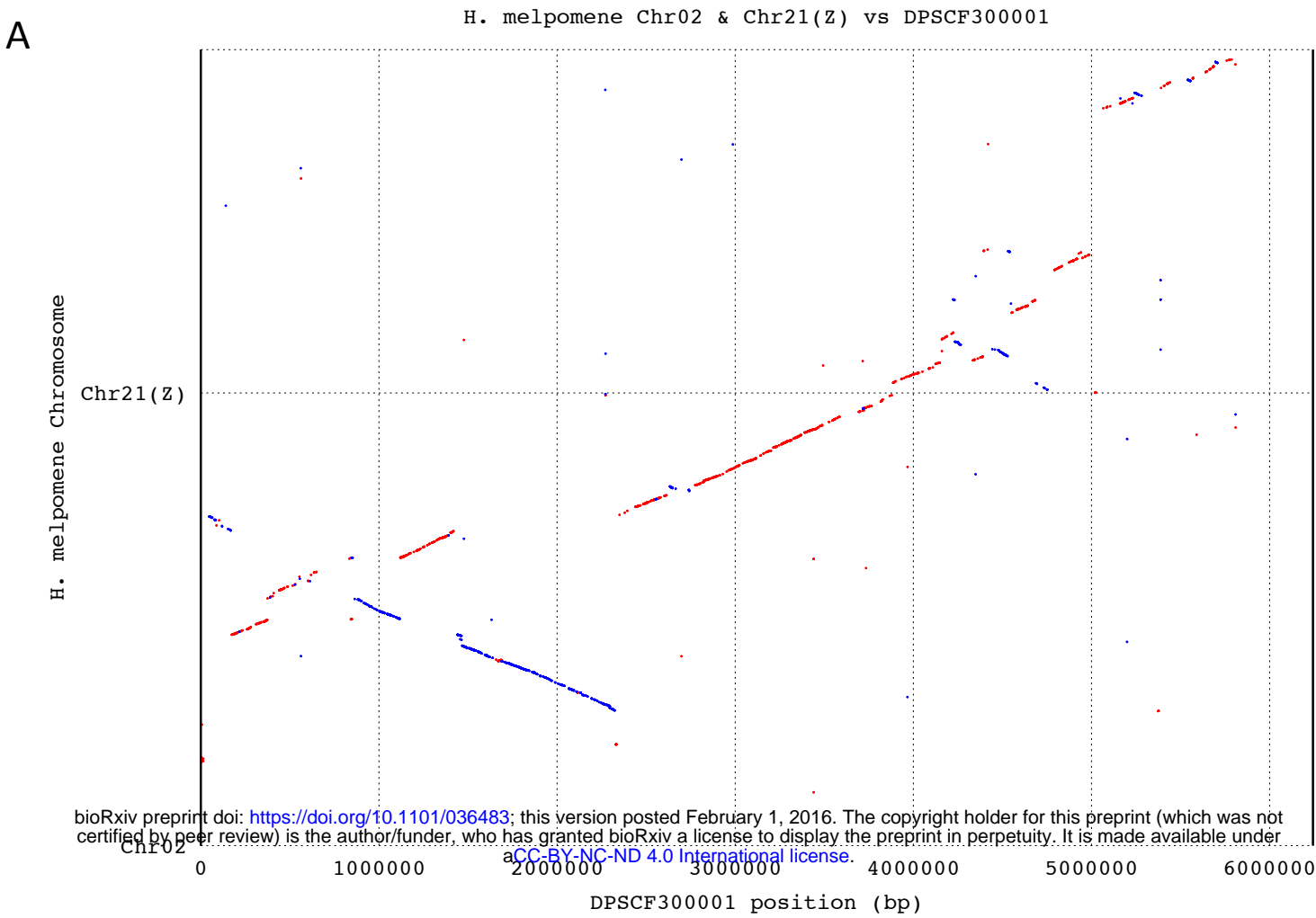


Figure S4. Promer alignments of DPSCF300001 against the Z and homologous autosome from (A) *H. melpomene* and (B) *M. cinxia*. Best one-to-one alignments were generated using default parameters. Manual inspection of alignment coordinates revealed the transition on DPSCF300001 from neo-Z to anc-Z occurs in a window between positions 3.878 and 3.886 Mbp.

Table S1. Summary of assigning *D. plexippus* genes and scaffolds to chromosomes via orthology “liftover” relative to three different reference assemblies.

<i>M. cinxia</i>	<i>H. melpomene</i>	<i>B. mori</i>	
15130	15130	15130	total number of protein coding genes in target
14129	14427	14566	number of target genes assigned to chromosome
0.934	0.954	0.963	fraction of target genes assigned to chromosome
454	514	508	number of target scaffolds assigned to chromosomes
6740	8190	7928	number of 1:1 orthologs identified
4607	7150	7534	number of 1:1 orthologs assigned to reference chromosome
0.684	0.873	0.95	fraction of 1:1 orthologs assigned to reference chromosome

Supplementary Table S2. Sample identification details for sequencing data used in covariate analyses.

Region	Sample	Species	Sex	Collecting location	Date	Accession
North America	Plex_MA_HI004_M	<i>plexippus</i>	male	Massachusetts, USA	July 3 2008	SRX679269
	Plex_MA_HI035_F	<i>plexippus</i>	female	Massachusetts, USA	August 10 2009	SRX679310
	Plex_FLn_StM123_F	<i>plexippus</i>	female	St. Marks, Florida, USA	October 2008	SRX680105
	Plex_FLn_StM146_M	<i>plexippus</i>	male	St. Marks, Florida, USA	October 2009	SRX681753
	Plex_WSM_M36_M	<i>plexippus</i>	male	Samoa	June 2007	SRX680118
	Plex_WSM_M38_F	<i>plexippus</i>	female	Samoa	June 2007	SRX681528
Other <i>Danaus</i>	Erip_BRA_16005_F	<i>erippus</i>	female	Brazil	September 2010	SRX682069
	Erip_BRA_16008_M	<i>erippus</i>	male	Brazil	September 2010	SRX682070
	Eres_CRC_92_F	<i>eresimus</i>	female	Costa Rica	July 24 2010	SRX682071
	Eres_FL_27_M	<i>eresimus</i>	male	Florida, USA	July 20 2009	SRX682072
	Gili_CRC_30_M	<i>gilippus</i>	male	Costa Rica	July 24 2010	SRX682073
	Gili_TX_01_F	<i>gilippus</i>	female	Texas, USA	October 2010	SRX998564